

## Magnetosonic Waveguide Model of Solar Wind Flow Tubes

A. K. Srivastava\* & B. N. Dwivedi\*\*

*Department of Applied Physics, Institute of Technology, Banaras Hindu University, Varanasi 221 005, India.*

\**e-mail: aks.astro.itbhu@gmail.com*

\*\**e-mail: bholadwivedi@yahoo.com*

**Abstract.** We consider solar wind flow tubes as a magnetosonic waveguide. Assuming a symmetric expansion in edges of slab-modelled waveguide, we study the propagation characteristics of magnetosonic wave in the solar wind flow tubes. We present the preliminary results and discuss their implications.

*Key words.* Solar wind—MHD waves—magnetic flux tubes.

### 1. Introduction

Parker's assumption (1963) that the solar wind may be fine-structured in the form of flow tubes has also been supported by the HELIOS spacecraft observations (Thieme *et al.* 1990). The wave propagation characteristics in such a magnetically-structured and inhomogeneous medium have been investigated by Roberts (1981a, b). Magnetosonic waves may be trapped in solar wind flow tubes assuming Alfvén speed to be less inside the tube than outside. The presence of the minimum Alfvén speed is required for trapping the waves. This is also correct in a low- $\beta$  plasma. The trapping of waves can also be caused by the discontinuity of the flow. So, the structures may support the propagation of trapped magnetosonic waves with stable transversal structures determined by the boundary conditions (Nakariakov *et al.* 1996). The trapping of magnetosonic waves are due to reflection of waves from the tangential discontinuity of plasma velocity or due to sudden variation of Alfvén or sound speed. Surface magnetosonic wave is evanescent both inside and outside of waveguide, while the body magnetosonic wave is oscillatory inside the waveguide and evanescent outside. Both the wave modes are localized and non-leaky.

Nakariakov *et al.* (1996) corrected the boundary conditions reported by Mann *et al.* (1992) and have considered the steady flow inside and outside waveguide to study the properties of trapped linear magnetosonic waves and also described the excitations of different modes of magnetosonic waves within the solar wind flow tubes. Joarder *et al.* (1996) have also studied the magnetosonic modes of magnetic structures in the presence of inhomogeneous steady flows. Joarder and Narayanan (2000) have examined the combined effect of non-parallel propagation and steady shear flows on the properties of hydromagnetic surface waves. Considering the non-parallel propagation of magnetosonic waves, Joarder (2002) have investigated these waves in the observed fine structures of high-speed solar wind streams. In this paper, we study the propagation

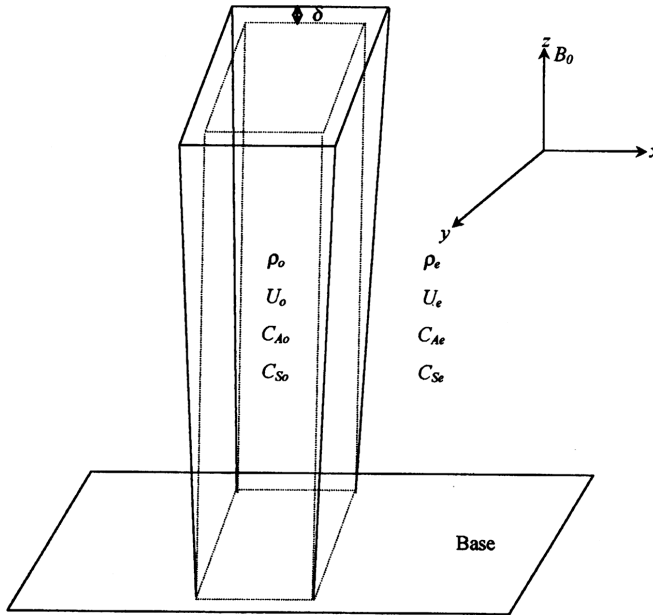


Figure 1. The solar wind flow tube model.

properties of magnetosonic waves. We also consider a symmetric expansion ( $\delta$ ) in the edges of the slab and its effect on propagation properties. We have studied the effect of magnetic field geometry of solar wind flow tubes on the propagation properties of different trapped modes of magnetosonic waves. Our solar wind flow tube model is more general in the sense that it supports both the body and surface magnetosonic waves. Each of the type of waves is also classified as kink and sausage modes.

### 2. Waveguide model and dispersion relation

We consider a magnetic slab with finite dimension  $x = \pm d$  and  $y = \pm d$ , having a background magnetic field in the  $z$ -direction, assuming the slab to be infinitely long. The steady shear flow along the  $z$ -axis are  $U_0$  and  $U_e$  for inside and outside the medium respectively. The sound speeds are  $C_{S0}$  and  $C_{Se}$  for inside and outside the slab respectively and similarly Alfvén speeds are  $C_{A0}$  and  $C_{Ae}$ . Plasma densities are  $\rho_0$  and  $\rho_e$  inside and outside the slab respectively.

We consider a symmetric expansion in the edges of the slab ( $\delta$ ) (Fig. 1). This follows the flux conservation law

$$B_{0z}A_{0z} = B_zA_z, \tag{1}$$

where  $B_{0z}$  and  $B_z$  are magnetic fields at the base and at any arbitrary height of the slab respectively. The respective cross-sectional areas of the slab are  $A_{0z}$  and  $A_z$ .

Using equation (1) and the slab geometry shown in Fig. 1, we get

$$\delta = \pm \frac{B_{0z}d^2}{B_z} - \frac{d^2}{4d}. \tag{2}$$

Using the dimensionless parameter  $d \approx 1$ , we have

$$\delta = \pm \frac{B_{0z} - B_z}{4B_z}. \quad (3)$$

$\delta$  represents an areal expansion of the slab at any height which may affect the transversal velocity structure both inside and outside the slab and can be incorporated in the coordinates. The positive sign in equations (2, 3) corresponds to divergent magnetic field lines geometry while the negative sign corresponds to convergent magnetic field lines geometry in our solar wind flow tubes model. We used only  $+\delta$  in our calculations, i.e., divergent magnetic field lines geometry of solar wind flow tubes. We have studied the effect of this magnetic field geometry on the propagation properties of magnetosonic wave modes.

The linearized MHD equations for ideal MHD give the following differential equation for inside and outside the slab (cf., Mann *et al.* 1992; Nakariakov *et al.* 1996).

$$\frac{d^2 V_{xi}}{dx^2} - m_i^2 V_{xi} = 0, \quad (4)$$

where  $i$  is either for inside or for outside the slab. The transversal plasma velocity is  $V_{xi}(x) \exp i(\omega t - kz)$ , and

$$m_i^2 = \frac{[a_{Ai}^2 - (a - M_i)^2][a_{Si}^2 - (a - M_i)^2]}{a_{fi}^2 [a_{Ti}^2 - (a - M_i)^2]} k^2, \quad (5)$$

where,

$$a = \frac{\omega}{kC_{A0}}; \quad a_{Ai}^2 = \frac{C_{Ai}^2}{C_{A0}^2}; \quad a_{Si}^2 = \frac{C_{Si}^2}{C_{A0}^2};$$

$$M_i = \frac{U_i}{C_{A0}}; \quad a_{Ti}^2 = \frac{C_{Ai}^2 C_{Si}^2}{C_{A0}^2 (C_{Ai}^2 + C_{Si}^2)}; \quad a_{fi}^2 = \frac{C_{Ai}^2 + C_{Si}^2}{C_{A0}^2}.$$

All variables are normalized with  $C_{A0}$ ,  $M_i$  is Alfvén Mach number and  $a$  is phase speed in units of Alfvén speed  $C_{A0}$ .  $a$  is the phase speed of different magnetosonic modes. Boundary conditions are as follows (cf., Nakariakov *et al.* 1996):

$$\frac{V_{x0}(x = \pm d)}{\omega - kU_0} = \frac{V_{xe}(x = \pm d)}{\omega - kU_e}, \quad (6a)$$

$$p_{To}(x = \pm d) = p_{Te}(x = \pm d) \quad (6b)$$

and

$$p_{Ti}(x) = \frac{iC_{A0}\rho_i a_{fi}^2 [a_{Ti}^2 - (a - M_i)^2] dV_{xi}}{k(a - M_i)[a_{Si}^2 - (a - M_i)^2] dx}. \quad (6c)$$

The solutions for the transversal structures of modes outside the slab in our model are given by,

$$V_{xe}(x) = \left\{ \begin{array}{ll} A_1 \exp[-m_e(x \pm \delta - d)], & x > d \\ A_2 \exp[+m_e(x \pm \delta + d)], & x < d \end{array} \right\}, \quad (7)$$

where  $A_1$  and  $A_2$  are constants. This equation is valid only in the case when the wavelength of the perturbation is much shorter than the characteristic spatial scale of the tube expansion according to the WKB approximation.

Solutions inside the slab for surface and body waves are:

$$V_{x0}(x) = \left\{ \begin{array}{ll} A \sinh[m_0(x \pm \delta)], & \text{for sausage surface modes} \\ A \cosh[m_0(x \pm \delta)], & \text{for kink surface modes} \\ A \sin[n_0(x \pm \delta)], & \text{for sausage body modes} \\ A \cos[n_0(x \pm \delta)], & \text{for kink body modes} \end{array} \right\}, \quad (8)$$

where  $A$  is constant and  $n_0^2 = -m_0^2$ .

We have taken  $M_e = 0$  and  $M_0 \rightarrow M$  because we have considered in our calculations the frame of reference related to the external flow. The  $M$  value is given by  $M = (U_0 - U_e)/C_{A0}$  which represents the difference between Alfvén Mach number inside and outside of solar wind flow tubes. Some unspecified acceleration mechanism is likely to be present inside flow tubes, so we have taken the constant value of steady flow. Nakariakov *et al.* (1996) also used the same approach in his calculations related to excitations of body magnetosonic waves in solar wind flow tubes. Applying the boundary conditions (6) on solutions given by equations (7–8), we also consider the incompressible plasma ( $\gamma \rightarrow \infty$ ), for which  $m_0$  (or  $n_0$ ) and  $m_e$  tends to  $k$ . We get the following dispersion relations for surface magnetosonic waves:

$$\left[ \tanh(kd \pm k\delta) + \frac{\rho_e}{\rho_0} \right] a^2 - 2Ma \tanh(kd \pm k\delta) + (M^2 - 1) \tanh(kd \pm k\delta) - \frac{\rho_e}{\rho_0} a_{Ae}^2 = 0, \quad \text{for kink surface wave} \quad (9)$$

and

$$\left[ \coth(kd \pm k\delta) + \frac{\rho_e}{\rho_0} \right] a^2 - 2Ma \coth(kd \pm k\delta) + (M^2 - 1) \coth(kd \pm k\delta) - \frac{\rho_e}{\rho_0} a_{Ae}^2 = 0, \quad \text{for sausage surface wave.} \quad (10)$$

When plasma  $\beta$  is small, then the Alfvén wave exceeds the sound speed. Surface mode may or may not exist for low- $\beta$  plasma. There cannot be two-sided surface waves in a low- $\beta$  plasma and it will not hold if only one side of the magnetic interface has a low- $\beta$  (Roberts 1981a; Wentzel 1979). That means the existence of one-sided normal modes of surface waves. Under this limit following two relations given for single normal mode of body waves, which may excite due to tangential discontinuity.

$$\left[ \tan(kd \pm k\delta) \pm \frac{\rho_e}{\rho_0} \right] a^2 - 2Ma \tan(kd \pm k\delta) + (M^2 - 1) \tan(kd \pm k\delta) - \frac{\rho_e}{\rho_0} a_{Ae}^2 = 0, \quad \text{for kink body waves} \quad (11)$$

and

$$\left[ \frac{\rho_e}{\rho_0} - \cot(kd \pm k\delta) \right] a^2 + 2Ma \cot(kd \pm k\delta) + (1 - M^2) \cot(kd \pm k\delta) - \frac{\rho_e}{\rho_0} a_{Ae}^2 = 0, \quad \text{for sausage body waves.} \quad (12)$$

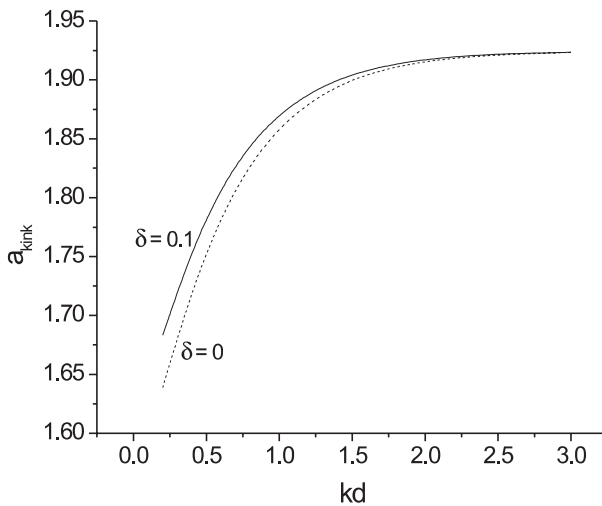
Dimensionless parameter  $(kd \pm k\delta)$  in degree ( $^\circ$ ), is employed in equations (9–12).

### 3. Magnetic slab with flow

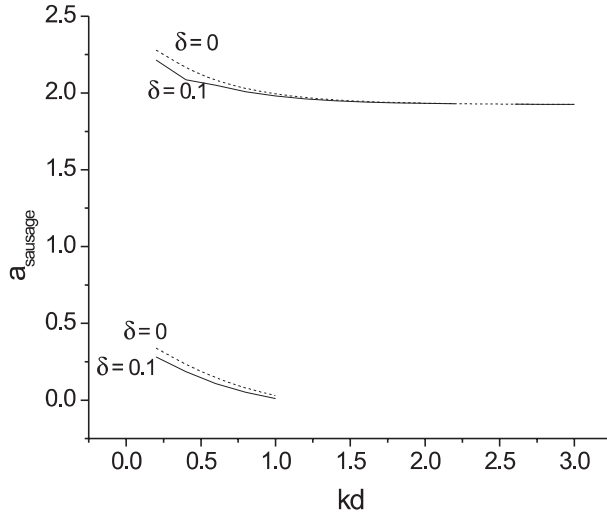
We have considered a flow ( $M = 1.46$ ) and actual solar-wind data of Thieme *et al.* (1990). We have used the parameters of solar wind flow tubes, Alfvén speed inside solar wind flow tubes  $C_{Ao} = 65 \text{ km s}^{-1}$ , sound speed inside solar wind flow tubes  $C_{So} = 65 \text{ km s}^{-1}$ , outside of flow tubes Alfvén speed  $C_{Ae} = 100 \text{ km s}^{-1}$  and sound speed  $C_{Se} = 70 \text{ km s}^{-1}$ . Steady flow inside of flow tubes  $U_0 = 750 \text{ km s}^{-1}$  and outside it  $U_e = 655 \text{ km s}^{-1}$ .  $\rho_e/\rho_0 = 0.583$ ,  $a_{Ae}^2 = 2.37$ ,  $d = 1.6 \times 10^6 \text{ km}$  are also used in our calculations. Figure 2 shows increasing phase velocity pattern for kink-surface modes. The phase velocities are greater for expanded tubes compared to the uniform magnetic flux-tubes. However, the flux-tube geometry does not have any effect at lower wavelengths.

Figure 3 shows two sausage surface modes. This could possibly be categorized as fast sausage surface wave and slow sausage surface wave. The lower limit of the fast sausage surface wave is  $(a_{A0} + M)$ . The upper limit of slow sausage surface wave is found at  $(M - a_{Se})$ . The effect of boundary perturbations is decreased for the phase velocities of two kinds of surface-sausage waves, but not affected at lower wavelengths.

Figures 4 and 5 show the phase velocity pattern of kink and sausage body waves respectively. Both the modes exhibit the increasing phase velocity pattern with velocities of two types of modes. We have plotted the phase speeds ( $a$ ) of kink and sausage



**Figure 2.** Dispersion curves for kink mode of surface magnetosonic wave in magnetic slab with flow ( $M = 1.46$ ).



**Figure 3.** Dispersion curves for sausage mode of surface magnetosonic wave in magnetic slab with flow ( $M = 1.46$ ).

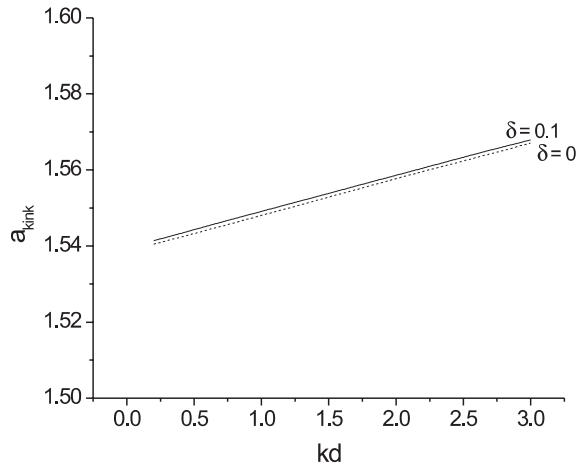


**Figure 4.** Dispersion curves for kink mode of body magnetosonic wave in magnetic slab with flow ( $M = 1.46$ ).

modes of surface and body magnetosonic waves with respect to  $kd$  in Figs. 2–5.  $kd$  is a dimensionless number. Since waveguide approach supports waves having wavelengths of the order of  $d$  or greater than  $d$  (i.e.,  $\lambda \geq d$ ), so the wave number  $k$  multiplied by  $d$  yields a dimensionless number.

#### 4. Concluding remarks

We have studied the propagation characteristics of different modes of magnetosonic waves, considering a magnetic slab with different outside and inside steady flows. We

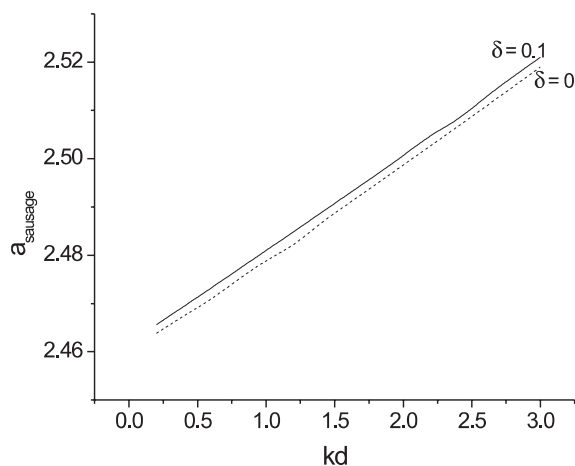


**Figure 5.** Dispersion curves for sausage mode of body magnetosonic wave in magnetic slab with flow ( $M = 1.46$ ).

also considered a symmetric expansion in edges of the slab at any arbitrary height. We find that surface waves may exist due to magnetic field discontinuity. When we approximated the tube embedded in plasma with different plasma- $\beta$  inside the tube, we see that it supports the existence of surface waves. We also find one normal and single mode of body wave due to tangential discontinuity and we have not considered higher modes of compressible plasma. With steady flow ( $M = 1.46$ ), kink mode velocity increases as  $kd$  increases while sausage mode of surface wave exhibits decreasing velocity pattern with  $kd$ . In case of sausage modes with flow, two modes exist. The first has a lower limit of phase speed ( $a_{A0} + M$ ) while the second has an upper limit of phase speed ( $M - a_{se}$ ). These may be categorized as fast and slow modes. Kink and sausage body waves show increasing velocity pattern. The ' $\delta$ ' factor does not affect the phase velocities, particularly at higher wave number.

### Acknowledgements

We are indebted to both the anonymous referees for their helpful comments.

### References

- Joarder, P. S., Nakariakov, V. M., Roberts, B. 1997, *Solar Phys.*, **176**, 285.  
 Joarder, P. S., Narayanan, A. S. 2000, *Astron. Astrophys.*, **359**, 1211.  
 Joarder, P. S. 2002, *Astron. Astrophys.*, **384**, 1086.  
 Mann, G., Marsch, E., Roberts, B. 1992, *Solar Wind Seven*, (eds.) Marsch, E., Schwenn, R., COSPAR Pergamon Press, 495.  
 Nakariakov, V. M., Roberts, B., Mann, G. 1996, *Astron. Astrophys.*, **311**, 311.  
 Parker, E. N. 1963, *Interplanetary Dynamical Processes*, Interscience, New York.  
 Roberts, B. 1981a, *Solar Phys.*, **69**, 27.  
 Roberts, B. 1981b, *Solar Phys.*, **69**, 39.  
 Thieme, K. M., Marsh, E., Schwenn, R. 1990, *Ann. Geophys.*, **8**, 713.  
 Wentzel, D. G. 1979, *Astrophys. J.*, **227**, 319.